Digital Camera-based Eye Movement Assessment Method for NeuroEye Examination

Mohamed Abul Hassan [1]

[1]Affiliation not available

October 30, 2023

Abstract

In this article, I/We report a novel eye-movement assessment method using a digital camera to measure eye conjugacy in healthy individuals while performing a neurological examination. This is clinically significant because this approach overcomes the limitations of complex and expensive setups (e.g., infrared cameras) that often make it impractical to scale up and translate to clinical use. Moreover, this approach removes the need for a calibration procedure which has caused prior studies to exclude participants, potentially introducing selection bias and limiting generalizability. Our study suggests that this technology could be deployed for clinical use in the clinic or pre-hospital setting, including telemedicine or emergency medical services (EMS) encounters to detect neurological injury or diseases that cause neuro-ocular deficits, like stroke.

A Digital Camera-based Eye Movement Assessment Method for NeuroEye Examination

Mohamed Abul Hassan[1], Xuwang Yin[2,*], Yan Zhuang[2,*], Chad M. Aldridge[3], Timothy McMurry, Andrew M. Southerland[3], and Gustavo K. Rohde[1,2]

***Abstract*—The ability to perform quantitative and automated neurological assessment could enhance diagnosis and treatment in the pre-hospital setting, such as during telemedicine or emergency medical services (EMS) encounters. Such a tool could be developed by adapting clinically significant information such as symmetry of eye movement or conjugate eye movement. Here we describe a digital camera-based eye tracking method "NeuroGaze" to capture the symmetry of eye movement while performing neurological eye examination. The proposed method was developed based on detecting the center of the pupil for both eyes from a given video and measuring eye conjugacy by transforming the pupil center coordinates to relative gaze. The method was tested on 18 healthy volunteers while performing three neurological eye examinations[1]. We also compared our proposed approach to state-of-the-art digital camera-based eye-tracking methods and commercial off-the-shelf (COTS) eye trackers. NeuroGaze outperformed digital camera-based eye tracking methods by reporting a mean Spearman rank-order correlation coefficient of 0.85 for the H-test, 0.85 for the Dot-test, and 0.5 for the OKN-Test, and shows similarity in trends for the relative gaze trajectories with a noticeable offset in the scale of the relative gaze angle compared to COTS eye tracker (see Fig. 1). The study demonstrates that by using a pupil-center-based eye-tracking method, a digital camera can measure clinically relevant information regarding eye movement.**

***Index Terms*—Remote Health Monitoring; Conjugate Gaze; Pupil Detection; Gaze Tracking; Posterior Circulation Stroke**

I. Introduction

Abnormal eye alignment and motion can indicate the presence of neurological diseases. Abnormal eye movements are often indicators of an underlying neurological disease, like Alzheimer's and stroke. Alzheimer's disease affects about 910,000 adults aged 65 or older per year [1], and stroke is a leading cause of death and disability globally [2]. As a result, there is considerable interest in implementing eye-tracking technology to evaluate these and other neurological diseases [3]–[5].

Recent efforts [6]–[9] to deploy eye-tracking technology show successful use of commercially available eye trackers in the detection of saccades and quick-phases during eye movement. This approach requires expensive equipment with laboratory setups to achieve the accuracy and precision necessary to track eye gaze over a screen. Unfortunately, the significant requirements of the same approach often make it impractical to scale up and translate to clinical use. A possible solution to improve eye-tracking practicality and clinical use is the application of machine learning techniques. Various research groups have already attempted these techniques to track eye movements with digital cameras like those in laptops and smartphones [10], [11]. These attempts demonstrate promise with relatively good predictions of gaze coordinates in comparison to commercial eye trackers [12]–[14], but still need more development to become equivalent or replace commercially available eye trackers.

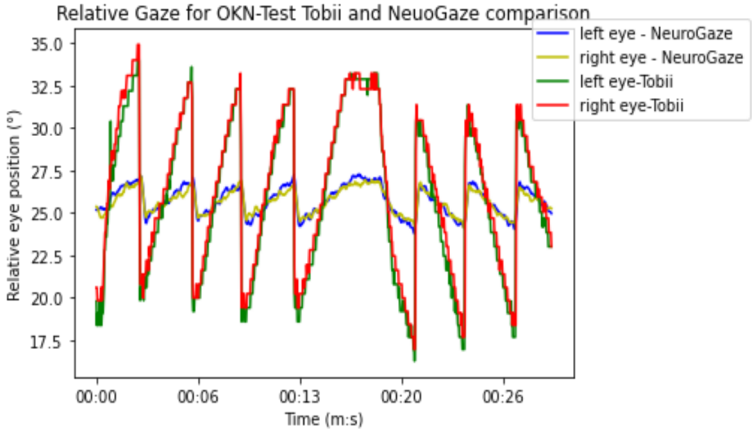

Fig. 1. Relative gaze plot comparison between Tobii and NeuroGaze for the OKN-Test

Given machine learning advancements in eye tracking for neurological diseases, these newer approaches [9], [15]–[17] attempt to replicate gaze coordinates. They often neglect to evaluate how the eyes move in tandem, which is an important component of a typical neurological exam. How the eyes move in tandem together is known as conjugacy. With a few congenital exceptions, humans have near-perfect eye conjugacy as a characteristic of normal physiology. (see Fig. 1). Conversely, a significant deviation or acquired loss of eye conjugacy is most often considered pathological [18]. For example, when the right eye can no longer move outward toward the temple, the eyes lose conjugacy as the person looks to the right since

[1] M. A. Hassan and G. Rohde are with the Imaging and Data Science Lab, Department of Biomedical Engineering, University of Virginia, VA 22903, USA.
[2] Y. Zhuang, X. Yin, and G. Rohde are with the Imaging and Data Science Lab, Department of Electrical and Computer Engineering, University of Virginia, VA 22903, USA.
[3] C. Aldridge, and A. Southerland are with the Department of Neurology, University of Virginia, VA 22903, USA.
[*] indicates that the authors contributed equally to the manuscript.

[1]The NeuroEye dataset is made available at https://www.kaggle.com/datasets/mahassan8/neuroeye

the left eye continues while the right eye remains still, unable to move. In this scenario, the differential diagnosis for a neurologist would include a brainstem stroke.

With the clinician's perspective in mind, we aim to determine the feasibility of digital camera-based eye trackers to measure eye conjugacy in healthy individuals by comparing the performance to COTS eye tracking equipment [19]. The details of our study arrange themselves in the following order: Section II discusses the related work in eye tracking. Section III presents the proposed method for digital camera-based eye movement assessment. Section IV presents the experimental setup used to perform the analysis. Section V and VI present the results and discussion of the digital camera-based eye movement assessment for NeuroEye. Section VII discusses the conclusive remarks of the study.

II. Related work

In general, video-based eye tracking systems can be categorized into model-based approaches and appearance-based approaches [20].

A. Model-based tracking systems

Model-based approaches often use one or more digital cameras to perform gaze estimation by using specific eye characteristics such as iris or pupil parameters to construct the 3D eye geometry model and determine the gaze points [21]. The most popular model-based methods use infrared sensors for imaging, including several available COTS [6], [22]. For example, medical research has used model-based eye trackers in several fields, such as ophthalmology [23], [24], psychiatry [25], psychology [26], psychopharmacology [27], and neurology [9], [15]–[17].

The COTS eye trackers have demonstrated use in analyzing pathological nystagmus [28], investigating gaze characteristics associated with autism [29], and classifying various visual field defects [24]. However, model-based methods are complex and expensive to set up (e.g., infrared cameras). A common element of these setups is a dedicated calibration procedure that must be performed prior to gaze tracking and estimation for each study participant. Multiple studies utilizing model-based methods in neurological disease research [9], [24], [30]–[35] had to exclude patients that cannot complete the calibration procedure. Excluding these patients leads to severe issues in the clinical generalizability of results and greatly reduces the practical use of these setups in clinical care.

B. Appearance-based tracking systems

Appearance-based methods often perform gaze estimation using a single digital camera. These methods directly model a mapping relationship between pupil positions from eye images and gaze points on the screen using learning-based techniques, such as linear regression [36] and neural networks [13], [37]. MPIIGaze is among the state-of-the-art gaze estimation methods [13], [38]. It is based on learning eye images and head orientation to predict gaze angles. The model is trained on the MPIIGaze dataset that learns from annotated screen coordinates.

Krafka et al. [14] proposed a different estimation method that uses a mobile phone/tablet camera. The process was based on a convolutional neural network (CNN) learning method using eye and face images and annotated screen coordinates to predict the screen coordinates at which the eyes focus. Huang et al. [39] proposed a regression-based learning method that used hand-crafted features from eye images. The features are input data for training and annotated screen coordinates. Park et al. [40] suggested a two-step learning process that learns from eye images to map gaze and its direction using a regression-based CNN. This method uses the eye images and the annotated screen coordinates as learning parameters to perform gaze direction predictions.

Detecting the pupil center to estimate screen coordinates is an alternative method that uses annotated screen coordinates; we have listed such recent implementations. Ahmed et al. [41] implemented an iris center localization approach by combining the circular gradient intensity with a CNN. This resulted in gaze estimation from the center of the iris. George et al. [42] implemented a geometrical eye center localization method dependent on fast convolution and ellipse fitting. Fabbian et al. [43] applied an eye center detection method by fitting a bounding box over the eyes. The localization of the gradient vector detected the pupil center within the bounding box. Similarly, Pauly et al. [44] used a bounding box extracted from the Haar cascade classifier and eye localization from histogram-oriented gradient features.

Using annotated screen coordinates as a learning parameter is a possible fit for fixation-based eye movement tasks. Neurophysiological studies [45], [46] reported involuntary triggering of eye movements from healthy individuals, such as catch up saccades of low gain while performing smooth pursuit eye movement tasks. These involuntary eye movements could affect the consistency of the screen coordinates annotation. Furthermore, annotating screen coordinates to capture the gaze depends on user feedback and, ultimately, the best effort of the participant. This is a potential limitation since multiple studies [47]–[49] indicate that participants may have varying attention spans to focus on the screen stimuli. Therefore, participants may not follow the stimuli consistently. To address some of these discussed issues, we aim to investigate further the impact of pupil detection methods using annotated pupil center coordinates and screen coordinates for gaze estimation in the clinical context.

III. Methods

The development of the proposed method has three main components described under the following subsections: 1) RoADIE, the apparatus used to acquire the data, 2) NeuroEye, a computer adaption of standard bedside clinical tests; and 3) NeuroGaze, the proposed method to quantify the conjugate eye movements. We hypothesized that a method developed for digital camera-based gaze estimation could demonstrate similar performance to a COTS eye-tracking device. Our

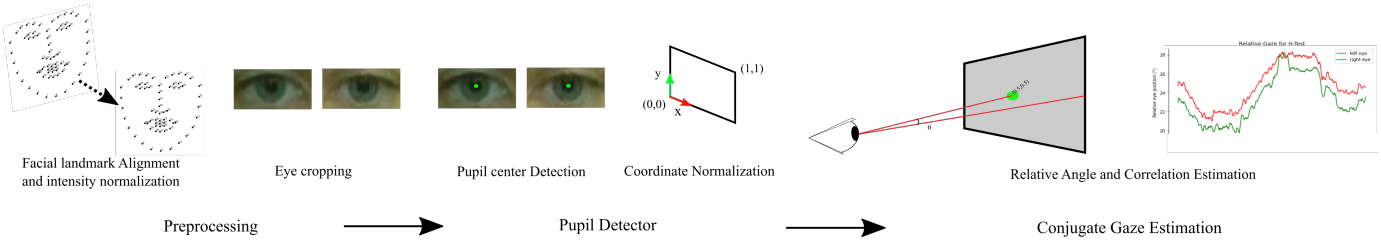

Fig. 2. Illustration of the proposed method: NeuroGaze

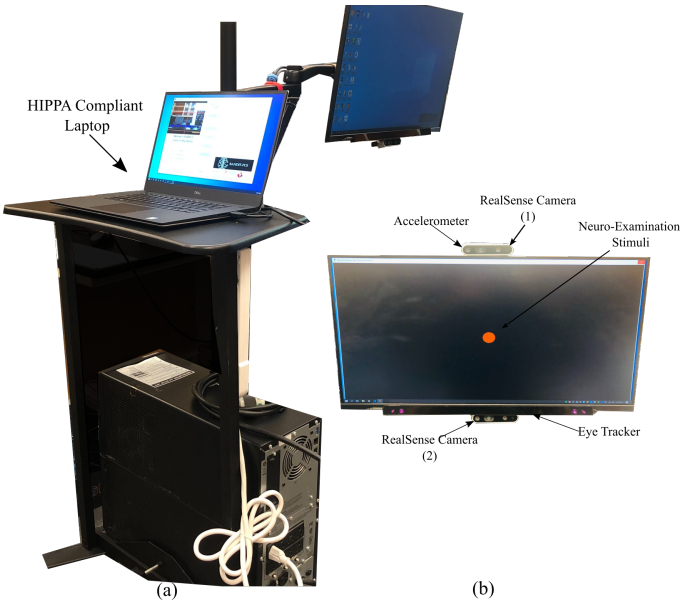

Fig. 3. Rolling Apparatus to Detect Impairment of the Eyes - RoADIE. (a) side view of the RoADIE mobile rig, (b) Illustration screen view including the hardware components for RoADIE

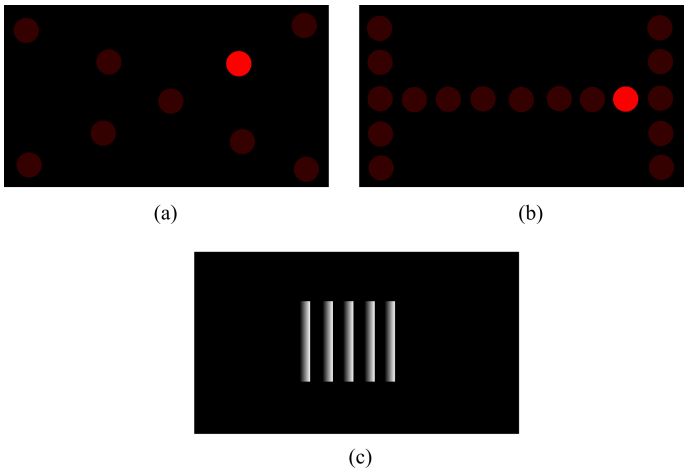

Fig. 4. Illustration of the NeuroEye examination. (a) represents the Dot-Test for the Neuro-eye examination. The red dot with the higher contrast represents the current position of the dot, and the red dot with the lower contrast represents the past, or future position of the dot (b) represents the H-Test for the Neuro-eye examination. The red dot with the higher contrast represents the current position of the dot, and the red dot with the lower contrast represents the past or future position of the dot (c) Illustration of the OKN-Test

proposed method uses a pupil detector to detect the center of the pupil for both eyes for a given video, then determine the conjugacy of the eye movement.

A. *RoADIE*

RoADIE (Rolling Apparatus for the Detection and Identification of Eye Movements) is a mobile rig we constructed to acquire data with the NeuroEye examination. The examination consists of three digitally adapted clinical neuro-ocular bedside tests. The RoADIE has a HIPPA-compliant computer to run our custom-built data acquisition software and to store the data. RoADIE has two digital cameras RealSense camera [50] embedded with RGB and infrared sensors. The RoADIE captures the gaze coordinates of the eyes using the "Tobii" Pro Fusion Eye Tracker [19]. The NeuroEye examination is displayed on the screen 0.6 meters from the participants. The sensor modalities' data acquisition is triggered globally with the activation of the examination session.

B. *NeuroEye*

The NeuroEye examination comprises three tests to examine various motor functionalities of the eye. The three tests are the "Dot-Test", "H-Test", and "OKN-Test", which are computer adaptions of standard bedside clinical tests [51]. The Dot Test is designed to assess the quality of eye coordination for each saccade. A clinician observes the movement of both eyes as the patient shifts their gaze from target to target (see Fig. 4 (a)). The clinician looks for the eyes to suddenly move to the next visual target and stop accurately at its destination. Abnormal signs include the eyes stopping short or too far away from the target, known as under or over-shooting, respectively, or the eyes do not initiate a saccade.

The H Test is designed to assess the quality of eye movement at a constant slow pace as the eyes track a visual target, smooth pursuit in all directions. The "H" pattern (see Fig. 4 (b)) ensures that both eyes track the target in all directions to their end ranges. Abnormal signs consist of the eyes lacking motion, or its initiation, in any direction or the eyes utilizing saccades to catch up to the moving visual target.

The optokinetic nystagmus (OKN) test measures an individual's ability to perform smooth pursuit, similar to the H test, and their ability to initiate a saccade to fixate on the following visual target after the first target disappears. The visual stimulus is typically vertical bars with high contrast

to the background. The bars move at a quick and constant pace from right to left (see Fig. 4 (c)). This is repeated in the opposite direction. OKN typically remains preserved in individuals with occipital lobe infarcts, with limited amplitude if there is a hemifield defect. Asymmetry in the performance of the eyes or poor ability to generate saccades may suggest damage to the optic, brainstem, or cerebellar nuclei or tracts.

C. NeuroGaze

NeuroGaze is our proposed method to quantify eye movements during the NeuroEye examination (see Fig. 2). The purpose of NeuroGaze is to provide physicians and healthcare workers with easy-to-interpret information regarding the patient's ability to perform conjugate eye movement. Our proposed method contains three main components (1) pre-processing, (2) pupil detection, and (3) conjugate gaze estimation.

1) Pre-processing: The RGB video stream from the RealSense camera was configured to capture the video of 1280×720 resolution at 30 fps. The stimuli of the H-test last for 24 seconds. Hence capturing 720 uncompressed frames during the examination. We used the "dlib" face detector [52] to extract facial landmarks to perform landmarks and intensity normalization that removes translation, rotation, and scale variations. Upon normalization, the left and right eyes were cropped from the face as separate images of 40×20 resolution using the facial landmark. The facial landmarks were also used to remove eye blink images. Blinking results in the movement of the eyelid that occludes the pupil. The vertical length ratio to the horizontal length is used to determine the blink.

2) Pupil Detection: Clinicians often follow the eye's iris and pupil center to assess the eye's ability to perform the conjugate movement. To mimic a clinician's perspective, we developed our pupil detector to locate *the center of the pupil*. The pupil center detector is parameterized by a convolutional neural network (CNN) and trained by minimizing the mean square error (MSE) between predicted pupil centers and ground truth pupil centers. The network consists (see Fig. 5) of two convolution layers (with kernel size 3×3) followed by two fully-connected layers. The last fully connected layer has two output nodes that are used for predicting the pupil center's x coordinate and y coordinate. We use the normalized coordinates to compute the MSE loss. The normalization is performed by dividing the original coordinate in the 20×40 coordinate system by 40 so that the normalized value falls in the $[0, 1]$ range. The network uses ReLU as the activation function.

We annotated 5400 pupil centers from here onwards, referred to as the "NeuroEye dataset" (see Figure 6(a) for examples). The NeuroEye dataset is made available at the project website[1]. The annotated pupil center images were accumulated by randomly selecting the left and right eye images for each participant for all three NeuroEye examinations. An Adam optimizer [53] of a learning rate of $5e-4$ is used

[1]https://www.kaggle.com/datasets/mahassan8/neuroeye

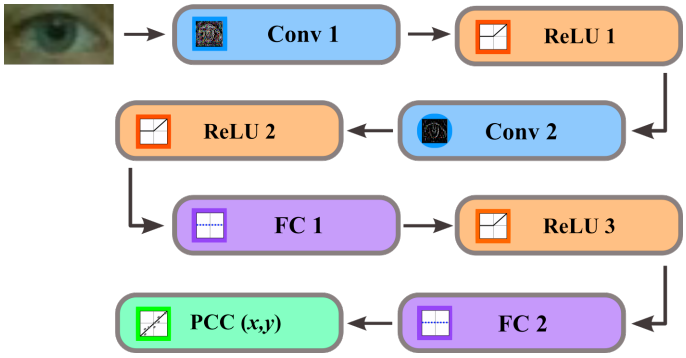

Fig. 5. Architecture of the CNN pupil center detector, comprised of two (Conv), Convolution layers, three (ReLU), ReLU activation functions, (FC) fully connected layers along with the output (PCC) pupil center coordinates.

for optimizing the model. To validate the effectiveness of the proposed pupil detection, we conducted a leave-one-out cross-validation (leave one patient's data for validation. and used other patients' data for training) and computed the l_1 distance between predicted and ground truth pupil center to quantify the prediction error, using $\frac{1}{N}\sum_{i=1}^{N}|s^i_{gth} - s^i_{pred}|_1$, where N is the total number of test eye images, s^i_{gth} is the ground truth pupil center location and s^i_{pred} is the predicted pupil center location. The mean error for 18 subjects is 0.805, with a standard deviation of 0.128. Fig. 6 shows pupil center ground truth annotations and test predictions.

3) Conjugate Gaze Estimation: We estimated the ability to perform conjugate eye movement by calculating the Spearman correlation coefficient r between the relative eye position of the left eye g_l and the right eye g_r using Eq. 1. The relative eye position is estimated from the "x", "y" coordinates of the pupil detector. We calculated the relative position of the eye using Eq. 2 to 4. Where θ_x and θ_y are the relative eye orientation on the x and y-axis. p_x and p_y are the normalized pupil center coordinates in the x and y-axis. a and b is the horizontal and vertical pixel range in the display screen (see Fig. 3 (b)). κ is the size of the pixel in the screen, d is the distance from the screen, and g is the relative eye position.

$$r = \frac{\sum_{i=1}^{n}(g_l - \bar{g_l})(g_r - \bar{g_r}))}{\sum_{i=1}^{n}(g_l - \bar{g_l})^2 \sum_{i=1}^{n}(g_r - \bar{g_r})^2} \tag{1}$$

$$\theta_x = atan(\frac{a \times p_x \times \kappa}{d}) \tag{2}$$

$$\theta_y = atan(\frac{b \times p_y \times \kappa}{d}) \tag{3}$$

$$g = \sqrt{\theta_x^2 + \theta_y^2} \tag{4}$$

IV. Experiment Setup

We designed the experiment to capture calibrated and non-calibrated gaze data using the Tobii eye tracker during separate sessions (please refer to [18] for details of the main experiment). University of Virginia's Institutional Review Board approved the study protocol. As such, the protocol complies

(a) Groundtruth annotations (b) Test predictions

Fig. 6. Pupil center ground truth annotations and test predictions for NeuroEye dataset

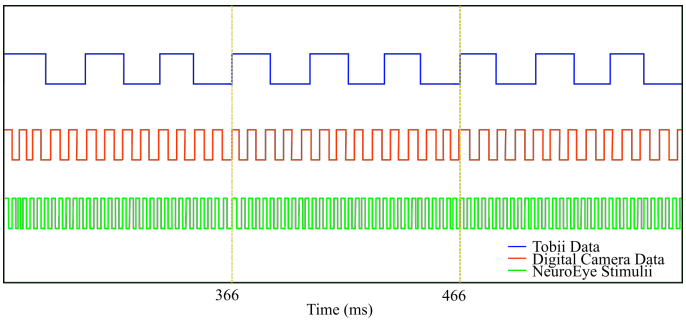

Fig. 7. Illustration of the data synchronization for RoADIE. The yellow guideline indicates the time point at which the data was extracted.

with all national ethical research standards in accordance with the Declaration of Helsinki. Written informed consent was obtained prior to subject enrollment and testing. Nineteen healthy controls participated in the calibration study. The mean age is 40 years consisting of 79 % female and 21 % male. The racial distribution of the controls was 81% White, 14% Asian, and 5% American Indian or Alaska Native. One participant did not follow the instructions during the experiment and was excluded from the study.

A. Data Synchronisation

During this study, we used the gaze data and the synchronized video from the RGB sensor of the RealSense Camera (1), which was acquired during the non-calibrated session. Further detail regarding non-calibrated gaze estimation using the Tobii eye tracker can be found here [18]. The Tobii eye tracker acquired data at 120 Hz, the digital camera acquired data at 30 Hz, and the NeuroEye simulations were set at 240 Hz. For a fair comparison, the data from the three sources were synchronized at 30 Hz during this study (see Fig. 7).

B. State-of-the-art

We evaluated the state-of-the-art, digital camera-based methods and our NeuroGaze prototype on the acquired NeuroEye examination video and compared it to the "Tobii" eye tracker. We used the video feeds during the NeuroEye examination as "input" for gaze estimation. The gaze estimations of the relative position of the left and right eyes were the "output". We substituted the Tobii gaze coordinates, the centroid of the Bounding Box coordinate, and the GazeML [54] screen coordinates to Eq. 1 to Eq. 4 to estimate the relative eye position for the left and right eye. We evaluated pre-trained implementations for MPIIGaze, and GazeML on NeuroEye Dataset since these two methods fundamentally predict the gaze points from annotated screen coordinates. The NeuroEye Dataset does not use labels/annotation for gaze points as screen coordinates. The screen coordinates of GazeML were accounted for and normalized for the relative gaze estimation. We used gaze orientation output from MPIIGaze [13], [38] implementation substituted to Eq. 4 to compute the relative gaze from the gaze orientation, and Eq. 1 to compute the conjugacy of the eye movement.

TABLE I
NEUROGAZE PUPIL DETECTOR MODEL DESCRIPTION

Pupil detector	Training	Testing
NeuroGaze (A)	NeruoEye	NeruoEye
NeuroGaze (B)	MPIIGaze-pupil center data	NeruoEye
NeuroGaze (C)	NeruoEye + MPIIGaze-pupil center data	NeruoEye

We performed a cross-dataset validation for a fair evaluation of NeuroGaze with the state-of-the-art methods above. Here we annotated pupil centers on a subset of the MPIIGaze dataset [55] and used the data in training the detection model of NeuroGaze. We annotated 2250 pupil center images by randomly selecting images of the left eye and right eye from each participant for each day. The implementations of NeuroGaze are as follows: "NeuroGaze (A)" trained on NeuroEye data and tested on NeuroEye data, "NeuroGaze (B)" trained on MPIIGaze-pupil center data and tested on NeuroEye data, and "NeuroGaze (C)" trained on NeuroEye and MPIIGaze-pupil center data and tested on NeuroEye data (see Table. I).

The methods [43], [44] developed for pupil center detection using a bounding box were dependent on non-generalized local variables and failed to perform effectively in the NeuroEye data. Therefore we developed a Bounding Box approach using a similar CNN architecture to NeuroGaze pupil center detection. The model consists of two convolution layers followed by two Relu activation layers of dimension $3 \times 20 \times 40$ and $32 \times 10 \times 20$ performing convolutions with a kernel of 3×3 and stride of 2. The third Relu activation layer is between two fully connected layers of dimension 3200×128 and 128×2. The final fully connected layer is connected to the Regression layer that outputs four nodes, respectively, used for the prediction of x, y, h, and w of the bounding box around the pupil center. The pupil center is estimated by estimating the centroid of the bounding box.

A total of 5400 bounding boxes around pupil centers were annotated to train and validate the Bounding Box pupil detector. The annotated pupil center images were accumulated from segments of 50 random images of the left and right eye for each participant performing the NeuroEye examinations: H-Test, Dot-Test, and OKN-Test. We trained the model to minimize the mean square error between the predicted and ground truth coordinates. An Adam optimizer [53] of a learning rate of $5e-4$ was used for model optimization.

C. Eye Conjugacy

We utilized the Spearman correlation coefficient to quantify the conjugacy of left and right gaze estimations obtained from the digital camera-based methods above. We chose the correlation coefficient because movement between the eye in humans has near "perfect coordination" [56]. This means that both eyes move at the same velocity in all directions. This is a de facto constant rate of change between the left and right eye, which results in a linear relationship. Mathematically a correlation coefficient represents this ocular physiology. Since the distribution of gaze coordinates is non-Gaussian, the Spearmen coefficient was preferred over Pearson.

V. Result

Table. II presents the overall performance of the camera-based eye-tracking methods for conjugate gaze estimation. For this analysis, we assumed that healthy participants could perform conjugate eye movement in all directions. This assumption was confirmed by the high Spearman rank correlation coefficient reported by the Tobii Eye tracker.

Among the digital camera-based methods, the NeuroGaze (A) reported the best conjugate gaze estimation with the highest mean correlation coefficient (see Table. II). The variations of the NeuroGaze method "NeuroGaze (B)", and "NeuroGaze (C)" also reported improved eye tracking performance compared to the state-of-the-art eye tracking methods. The GazeML method reported the lowest correlation coefficient mean for all three NeuroEye examinations. In general, digital camera-based eye-tracking methods reported a higher variability in eye tracking for different participants compared to the Tobii eye tracker (see Fig. 8).

The H-Test stimulates a motion across all the quadrants of the screen. The NeuroGaze (A) reported a correlation coefficient mean of 0.85 with a 95% confidence interval ranging from 0.59 to 0.93. The Bounding Box method reported a correlation coefficient mean of 0.72 with a 95% confidence interval ranging from 0.47 to 0.90. The MPIIGaze reported a correlation coefficient mean of 0.60 with a 95% confidence interval ranging from 0.33 to 0.81. The overall performance of digital camera-based eye tracking methods showed a 40% to 45% variability in conjugate gaze estimation (see Fig. 8).

The relative gaze plot for the H-Test shows (see Fig. 9) a highly conjugate eye movement between the left and right eye for Tobii. The NeuroGaze showed the most conjugate eye movement while tracking with a similar trajectory to the relative gaze trajectory of Tobii. The Bounding Box approach also showed a similar trajectory to the relative gaze trajectory of Tobii. However, the Bounding Box approach did not consistently capture the conjugacy of the eye movement since there was an offset in pupil center detection for both eyes. The MPIIGaze also showed evidence of following a similar trajectory to the relative gaze trajectory of Tobii. However, the MPIIGaze trajectory was inconsistent and did not capture the eye movement's conjugacy.

The Dot-Test stimulates a series of saccade and fixation eye movement events across all the quadrants of the screen canvas. The NeuroGaze (A) outperformed the state-of-the-art digital camera-based methods with a correlation coefficient mean of 0.85 with a 95% confidence interval ranging from 0.54 to 0.95 (see Table. II). The Bounding Box approach reported a correlation coefficient mean of 0.72 with a 95% confidence interval ranging from 0.27 to 0.86. The MPIIGaze reported a correlation coefficient mean of 0.55 with a 95% confidence interval ranging from 0.29 to 0.84. The pupil center-based eye tracking methods reported a tighter eye tracking variability of 20% to 25% (see Fig. 8).

The relative gaze plot for the Dot-Test shows (see Fig. 9) the relative eye movement during periods of fixation (when the relative gaze is flat) and saccade (when the relative gaze has a steep rise). NeuroGaze captured the most conjugate eye movement while tracking the fixation and saccade eye movement. The NeuroGaze showed a similar trajectory to the relative gaze trajectory of Tobii. The Bounding Box approach did not consistently capture the left and right eye movement. The conjugacy of eye movement was also reasonable during fixation periods. However, the ability to capture eye movement conjugacy lowered during periods of saccades.

The OKN-Test stimulates a series of alternative smooth pursuit and saccade eye movements resulting in a consistent movement of the eyes horizontally at two different speeds. The Tobii reported its lowest correlation coefficient mean of 0.84 among the three NeuroEye examinations for the OKN test. At the same time, Tobii eye tracking presented a variability of 25% among the healthy participants from the study. Among digital camera-based eye tracking, NeuroGaze (A) reported the highest performance with a correlation coefficient mean of 0.5 with a 95% confidence interval ranging from 0.41 to 0.74 (see Table. II). The Bounding Box approach reported a correlation coefficient mean of 0.38 with a 95% confidence interval ranging from 0.09 to 0.6. The MPIIGaze reported a correlation coefficient mean of 0.38 with a 95% confidence interval ranging from 0.13 to 0.61. Both COTS and digital camera-based eye tracker performance decreased during the OKN-Test.

The relative gaze plot for the OKN-Test shows that (see Fig. 9) the eye movement during periods of smooth pursuit (when the relative gaze has a linear rise) and saccades (when the relative gaze has a steep rise). The NeuroGaze outperformed other digital camera-based-eye tracking methods by capturing the most conjugate eye movement while tracking the smooth pursuit and saccade eye movement. The NeuroGaze also showed a similarity in trajectory to the relative gaze trajectory of Tobii. However, the Bounding Box approach showed a less similar trajectory to the relative gaze trajectory of Tobii. This could also result from the Bounding Box approach's inability to capture the left and right eye movement consistently.

VI. Discussion

In this preliminary study, we demonstrated the potential of digital camera-based methods to estimate eye movement and conjugacy. Conjugacy is a clinically relevant characteristic that neurologists and ophthalmologists utilize to determine the

TABLE II

MEAN CORRELATION AND THE 95% CONFIDENCE INTERVAL (CI) COMPARISON FOR THE SPEARMAN RANK-ORDER CORRELATION COEFFICIENT OF THE PROPOSED NEUROGAZE, COTS EYE TRACKER, AND STATE-OF-THE-ART DIGITAL CAMERA-BASED EYE-TRACKING METHODS

Method	H-Test		Dot-Test		OKN-Test	
	mean	95% CI	mean	95% CI	mean	95% CI
Tobii	0.95	(0.91,0.98)	0.96	(0.91,0.97)	0.84	(0.70,0.94)
Bounding Box	0.72	(0.47,0.90)	0.72	(0.27,0.86)	0.38	(0.09,0.60)
MPIIGaze	0.60	(0.33,0.81)	0.55	(0.29,0.84)	0.38	(0.13,0.61)
GazeML	0.14	(-0.09,0.33)	0.14	(-0.15,0.38)	0.12	(-0.01,0.38
NeuroGaze (A)	**0.85**	**(0.59,0.93)**	**0.85**	**(0.78,0.95)**	**0.50**	**(0.41,0.74)**
NeuroGaze (B)	0.79	(0.69,0.89)	0.79	(0.63,0.90)	0.45	(0.34,0.56)
NeuroGaze (C)	0.81	(0.73,0.91)	0.82	(0.77,0.90)	0.47	(0.10,0.75)

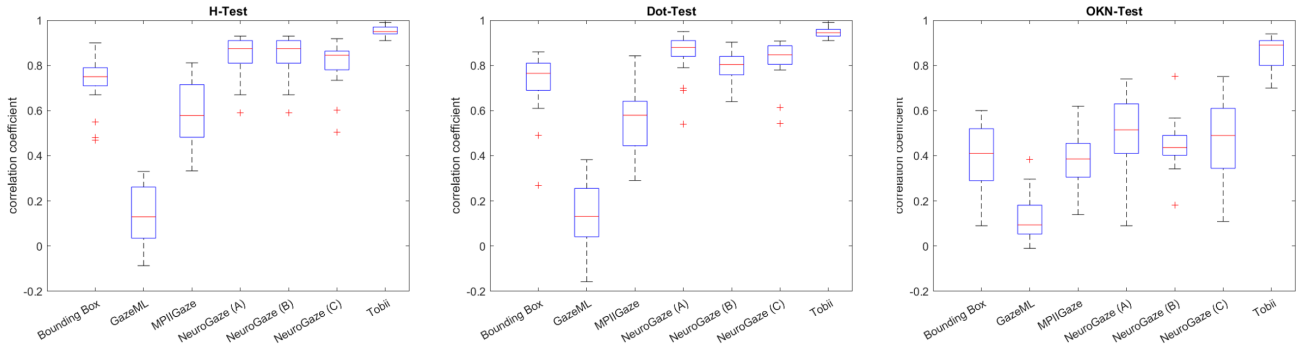

Fig. 8. Box-Whisker plot representation of the Spearman rank-order correlation coefficient summary of all participants for COTS eye tracker and state-of-the-art web camera-based eye-tracking methods

presence of neuropathology. To achieve this, we developed a novel method to investigate the performance of digital camera-based eye tracking during computer-adapted neurological eye examinations. Moreover, we highlighted the importance of eye-tracking methods using the pupil center to track the eyes based on annotated screen coordinates. We also showed the impact of relative gaze use and the generalizability of the pupil-center detection approach. The findings of this study highlight the feasibility of using a digital camera-based gaze estimation to measure clinically relevant eye-tracking information.

A. *Impact of Neurological Eye Examinations*

The previous implementation of eye tracking with a digital camera mainly measured gaze points, fixation sequence, heat maps, and area of interest [57], [58]. Neurological eye examinations stimulate or elicit fixation patterns, smooth pursuit, and saccadic eye movements. These clinically relevant measurements are widely different compared to conventional gaze measurements [58]. Eye conjugacy is one clinically relevant measurement estimated from binocular eye movements. The COTS and NeuroGaze eye conjugacy estimations were mainly affected during the OKN-test by continuous eye motion stimulated by smooth pursuit and saccadic eye movements. The low image acquisition speed of Tobii at 120 Hz and NeuroGaze at 30 Hz compared to the speed of saccadic movements may have impacted the quantification of eye conjugacy measurements during the OKN-test. The impact of image acquisition speed for NeuroGaze may be reflected in the variability in conjugacy measurements from H-test and Dot-Test (see Fig. 8). NeuroGaze reported a high variability during H-test in which the eye continuously moved at a physiologically slow speed, whereas low variability is present in the Dot-test in which the eyes switch from fixated and saccadic phases. The "stop" and "go" pattern of eye movement (Dot-test) is more suitable for NeuroGaze compared to continuous eye movement elicited during the H-test.

B. *Pupil Center*

We demonstrated that a digital camera could measure clinically relevant information using a pupil-center-based eye-tracking method. The method comprises multiple steps, including facial landmark alignment, normalization, and appearance-based pupil center detection. We showed that it is more advantageous to develop a model by training on pupil center coordinates compared to screen coordinates. Comparing the performance of the pre-trained MPIIGaze and GazeML on the NeuroEye dataset was unfair since the models were not trained on this dataset. For a fairer evaluation, we trained NeuroGaze (B) on the MPIIGaze dataset, then tested it on the NeuroEye dataset (see Fig. 10). NeuroGaze (B) still outperformed the MPIIGaze method, which further emphasizes appearance-based pupil detection's benefit in measuring eye conjugacy. Moreover, the performances of NeuroGaze A, B, and C training conditions suggest good generalizability of the three CNN models. Specifically, NeuroGaze (C), trained with the NeuroEye and tested on the MPIIGaze dataset, has the most adaptability among the three models.

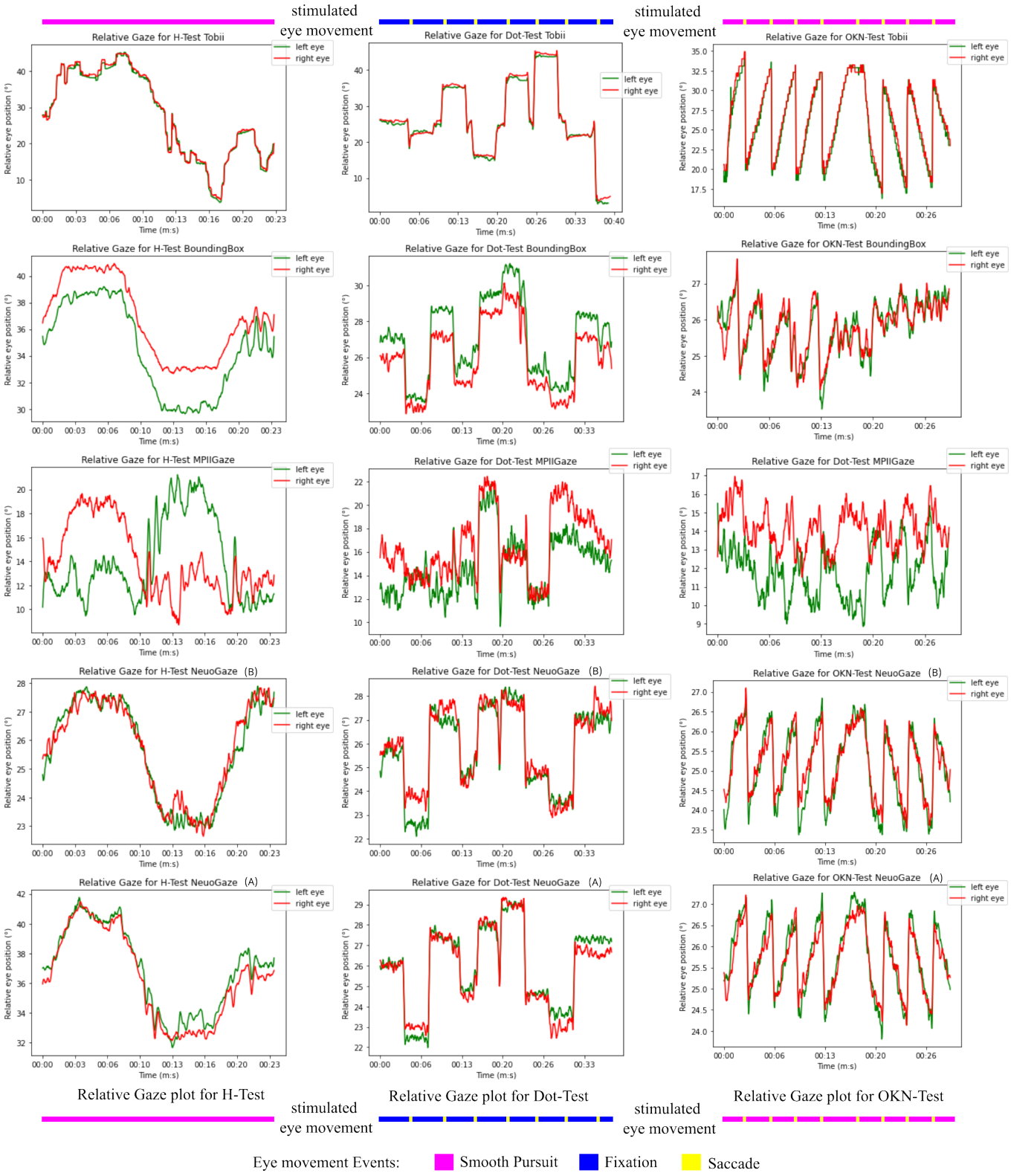

Fig. 9. Illustration of the relative gaze plot for a participant along with the eye movement stimulation indicators for the H-Test (row 1), Dot-Test (row 2), and OKN-Test (row 3) of the Tobii (column 1), Bounding Box(column 2), MPIIGaze (column 3), NeuroGaze B (column 4) and NeuroGaze A (column 5).

NeuroGaze (A) NeuroGaze (B) NeuroGaze (C)

Fig. 10. NeuroGaze Pupil Center detection on NeuroEye dataset. NeuroGaze (A) trained on NeuroEye data, NeuroGaze (B) trained on MPIIGaze-pupil center data, and NeuroGaze (C) trained on NeuroEye and MPIIGaze-pupil center data.

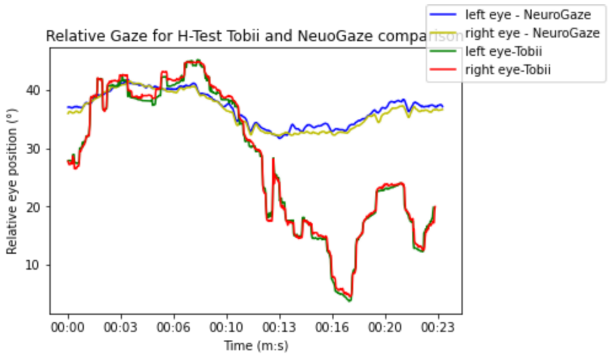

Fig. 11. Relative gaze plot comparison between Tobii and NeuroGaze for the OKN-Test

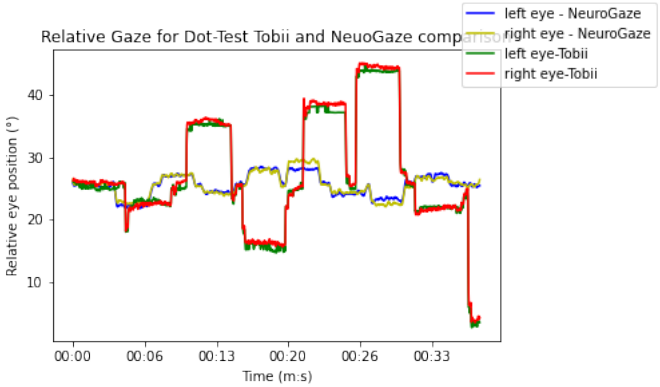

Fig. 12. Relative gaze plot comparison between Tobii and NeuroGaze for the Dot-Test

C. Relative Gaze Trajectory

In addition to quantifying the conjugacy, combining the relative gaze trajectory/path with eye movement detection methods [7], [59] enables the quantification of eye movement events such as the number of saccades performed during the OKN-test. This correlative information about the left and right eye may overcome the limitations caused by the slow image acquisition speeds of the digital camera as shown in relative gaze plots in Fig. 1 and Fig. 11.

D. NeuroGaze vs. Tobii

The relative gaze plots comparing Tobii and NeuroGaze show (see Fig. 1, 11, 12) that similar trends among the trajectories. The path plots also highlight the capability of NeuroGaze to capture fixation, smooth pursuit, and saccade eye movements. However, there is a clear difference in the scale of the relative gaze angle. The dissimilarity is most likely due to the different working principles of the COTS eye tracker "Tobii" and NueroGaze. The NeuroGaze works based on identifying the pupil center of the eye to estimate the relative gaze. This is achieved using the eye's optical axis to perform relative gaze estimation. Tobii, on the other hand, works on the principle of pupil central corneal reflection (PCCR) to estimate relative gaze [60]. PCCR is based on re-constructing the optical axis to derive the visual axis and estimate gaze using the visual axis. The difference between the optical and visual axis is known as the Kappa angle. Therefore, we can assume that the Kappa angle may be the most likely cause of the difference in scale of the relative gaze angle.

E. Limitations

There are a few limitations to this study. First, as a proof-of-concept, our study included small sample sizes and lacked race/ethnic diversity. The full extent of a gaze correlation coefficient to discriminate between normal and abnormal eye movements will require further research with larger and more diverse sample sizes and a greater range of neuro-ocular deficits. Despite the small sample size, it may be reasonable to assume that the healthy participants in this cohort represent the distribution of normal eye movements in a healthy adult population. We are currently collecting data on consecutive patients presenting with the acute vestibular syndrome and posterior circulation stroke to better assess the feasibility of NeuroGaze in a population with pathological eye movements.

The relative gaze plot of Tobii for the H-test (see Fig. 11) shows catch-up saccades of low gain while performing smooth pursuit eye movements. These small catch-up saccades are normal during smooth pursuits [61]. However, we noticed that the digital camera-based eye-tracking methods had limited ability to capture these small saccades consistently. We hypothesize that the slow image acquisition speed is why these methods miss small saccades.

VII. CONCLUSION

We investigated the feasibility of using a digital camera to capture eye movements during digitally adapted clinical eye exams (NeuroEye). We presented the performance of a novel method NeuroGaze along with other state-of-the-art digital camera-based eye tracking methods and compared them internally and to a COTS eye tracker. NeuroGaze demonstrated the ability to estimate eye conjugacy consistently better than other state-of-the-art methods, under fair comparison conditions. NeuroGaze did so by having the most similar conjugacy estimates to the "Tobii" reference and less variability. Specific to NeuroGaze, our method tested accurately for most participants of the H-Test and Dot-Test, and a few participants of the OKN-test. This is promising since NeuroGaze can be further improved to capture conjugate eye movements in these less accurate cases by (1) increasing the number of training samples by enrolling more participants and (2) improving the architecture of the pupil detector to achieve enhanced accuracy of measuring the pupil center.

In conclusion, we present preliminary evidence that digital cameras can be used with machine learning techniques to estimate eye conjugacy for future clinical applications. This is clinically significant because this approach overcomes the limitations of complex and expensive setups (e.g., infrared cameras). More importantly, this approach removes the need for a calibration procedure which has caused prior studies to exclude participants, potentially introducing selection bias and limiting generalizability. Our feasibility study suggests that this technology could be deployed for clinical use in the clinic or pre-hospital setting, including telemedicine or emergency medical services (EMS) encounters to detect neurological injury or diseases that cause neuro-ocular deficits, like stroke. This underscores the need for further research on this approach with neurological disease populations. This is the focus of our continued research.

REFERENCES

[1] MSG Monica Moore, Mirella Díaz-Santos, and Keith Vossel, "Alzheimer's association 2021 facts and figures report," .

[2] Mira Katan and Andreas Luft, "Global burden of stroke," in *Seminars in neurology*. Thieme Medical Publishers, 2018, vol. 38, pp. 208–211.

[3] Uiseo Nam, Kunyoung Lee, Hyunwoong Ko, Jun-Young Lee, and Eui Chul Lee, "Analyzing facial and eye movements to screen for alzheimer's disease," *Sensors*, vol. 20, no. 18, pp. 5349, 2020.

[4] Ling Tao, Quan Wang, Ding Liu, Jing Wang, Ziqing Zhu, and Li Feng, "Eye tracking metrics to screen and assess cognitive impairment in patients with neurological disorders," *Neurological Sciences*, pp. 1–8, 2020.

[5] Ying Gao and Bernhard A Sabel, "Microsaccade dysfunction and adaptation in hemianopia after stroke," *Restorative neurology and neuroscience*, vol. 35, no. 4, pp. 365–376, 2017.

[6] Agostino Gibaldi, Mauricio Vanegas, Peter J Bex, and Guido Maiello, "Evaluation of the tobii eyex eye tracking controller and matlab toolkit for research," *Behavior research methods*, vol. 49, no. 3, pp. 923–946, 2017.

[7] Sai Akanksha Punuganti and Jorge Otero-Millan PhD, "Detection of saccades and quick-phases in eye movement recordings with nystagmus," in *ACM Symposium on Eye Tracking Research and Applications*, 2020, pp. 1–5.

[8] Sai Akanksha Punuganti, Jing Tian, and Jorge Otero-Millan, "Automatic quick-phase detection in bedside recordings from patients with acute dizziness and nystagmus," in *Proceedings of the 11th ACM Symposium on Eye Tracking Research & Applications*, 2019, pp. 1–3.

[9] Deepesh Kumar, Anirban Dutta, Abhijit Das, and Uttama Lahiri, "Smarteye: developing a novel eye tracking system for quantitative assessment of oculomotor abnormalities," *IEEE Transactions on neural systems and rehabilitation engineering*, vol. 24, no. 10, pp. 1051–1059, 2016.

[10] T Maxwell Parker, Nathan Farrell, Jorge Otero-Millan, Amir Kheradmand, Ayodele McClenney, and David E Newman-Toker, "Proof of concept for an "eyephone" app to measure video head impulses," *Digital biomarkers*, vol. 5, no. 1, pp. 1–8, 2021.

[11] Mohamed Abul Hassan, Xuwang Yin, Yan Zhuang, Chad M Aldridge, Timothy McMurry, Andrew M Southerland, and Gustavo K Rohde, "A pilot study on video-based eye movement assessment of the neuroeye examination," in *2021 IEEE EMBS International Conference on Biomedical and Health Informatics (BHI)*. IEEE, 2021, pp. 1–4.

[12] Pingmei Xu, Krista A Ehinger, Yinda Zhang, Adam Finkelstein, Sanjeev R Kulkarni, and Jianxiong Xiao, "Turkergaze: Crowdsourcing saliency with webcam based eye tracking," *arXiv preprint arXiv:1504.06755*, 2015.

[13] Xucong Zhang, Yusuke Sugano, Mario Fritz, and Andreas Bulling, "Mpiigaze: Real-world dataset and deep appearance-based gaze estimation," *IEEE transactions on pattern analysis and machine intelligence*, vol. 41, no. 1, pp. 162–175, 2017.

[14] Kyle Krafka, Aditya Khosla, Petr Kellnhofer, Harini Kannan, Suchendra Bhandarkar, Wojciech Matusik, and Antonio Torralba, "Eye tracking for everyone," in *Proceedings of the IEEE conference on computer vision and pattern recognition*, 2016, pp. 2176–2184.

[15] Yasuo Terao, Hideki Fukuda, and Okihide Hikosaka, "What do eye movements tell us about patients with neurological disorders?â€"an introduction to saccade recording in the clinical settingâ€"," *Proceedings of the Japan Academy, Series B*, vol. 93, no. 10, pp. 772–801, 2017.

[16] Akane Oyama, Shuko Takeda, Yuki Ito, Tsuneo Nakajima, Yoichi Takami, Yasushi Takeya, Koichi Yamamoto, Ken Sugimoto, Hideo Shimizu, Munehisa Shimamura, et al., "Novel method for rapid assessment of cognitive impairment using high-performance eye-tracking technology," *Scientific reports*, vol. 9, no. 1, pp. 1–9, 2019.

[17] Daniel S Asfaw, Pete R Jones, Laura A Edwards, Nicholas D Smith, and David P Crabb, "Using eye movements to detect visual field loss: a pragmatic assessment using simulated scotoma," *Scientific reports*, vol. 10, no. 1, pp. 1–13, 2020.

[18] Mohamed Abul Hassan, Chad M Aldridge, Yan Zhuang, Xuwang Yin, Timothy McMurry, Gustavo K Rohde, and Andrew M Southerland, "Approach to quantify eye movements to augment stroke diagnosis with a non-calibrated eye-tracker," *IEEE Transactions on Biomedical Engineering*, 2022.

[19] Tobii AB, "Tobii pro fusion," Tech. Rep., Tobii Pro Inc., 2019.

[20] Dan Witzner Hansen and Qiang Ji, "In the eye of the beholder: A survey of models for eyes and gaze," *IEEE transactions on pattern analysis and machine intelligence*, vol. 32, no. 3, pp. 478–500, 2009.

[21] Elias Daniel Guestrin and Moshe Eizenman, "General theory of remote gaze estimation using the pupil center and corneal reflections," *IEEE Transactions on biomedical engineering*, vol. 53, no. 6, pp. 1124–1133, 2006.

[22] Frans W Cornelissen, Enno M Peters, and John Palmer, "The eyelink toolbox: eye tracking with matlab and the psychophysics toolbox," *Behavior Research Methods, Instruments, & Computers*, vol. 34, no. 4, pp. 613–617, 2002.

[23] William Rosengren, Marcus Nyström, Björn Hammar, and Martin Stridh, "A robust method for calibration of eye tracking data recorded during nystagmus," *Behavior research methods*, pp. 1–15, 2019.

[24] Alessandro Grillini, Daniel Ombelet, Rijul S Soans, and Frans W Cornelissen, "Towards using the spatio-temporal properties of eye movements to classify visual field defects," in *Proceedings of the 2018 ACM Symposium on Eye Tracking Research & Applications*, 2018, pp. 1–5.

[25] Roy S Hessels, Richard Andersson, Ignace TC Hooge, Marcus Nyström, and Chantal Kemner, "Consequences of eye color, positioning, and head movement for eye-tracking data quality in infant research," *Infancy*, vol. 20, no. 6, pp. 601–633, 2015.

[26] Lucas Paletta, Martin Pszeida, Amir Dini, Silvia Russegger, Sandra Schuessler, Anna Jos, Eva Schuster, Josef Steiner, and Maria Fellner, "Mira–a gaze-based serious game for continuous estimation of

alzheimer's mental state," in *ACM Symposium on Eye Tracking Research and Applications*, 2020, pp. 1–3.

[27] Charlotte JW Connell, Benjamin Thompson, Jason Turuwhenua, Robert F Hess, and Nicholas Gant, "Caffeine increases the velocity of rapid eye movements in unfatigued humans," *Psychopharmacology*, vol. 234, no. 15, pp. 2311–2323, 2017.

[28] Daniela Giordano, Carmelo Pino, Concetto Spampinato, Massimo Di Pietro, and Alfredo Reibaldi, "Eye tracker based method for quantitative analysis of pathological nystagmus," in *2011 24th International Symposium on Computer-Based Medical Systems (CBMS)*. IEEE, 2011, pp. 1–6.

[29] Mayada Elsabbagh, Evelyne Mercure, Kristelle Hudry, Susie Chandler, Greg Pasco, Tony Charman, Andrew Pickles, Simon Baron-Cohen, Patrick Bolton, Mark H Johnson, et al., "Infant neural sensitivity to dynamic eye gaze is associated with later emerging autism," *Current biology*, vol. 22, no. 4, pp. 338–342, 2012.

[30] William Rosengren, Marcus Nyström, Björn Hammar, and Martin Stridh, "Suitability of calibration polynomials for eye-tracking data with simulated fixation inaccuracies," in *Proceedings of the 2018 ACM Symposium on Eye Tracking Research & Applications*, 2018, pp. 1–5.

[31] Zhe Zeng, Felix Wilhelm Siebert, Antje Christine Venjakob, and Matthias Roetting, "Calibration-free gaze interfaces based on linear smooth pursuit," *Journal of Eye Movement Research*, vol. 13, no. 1, pp. 3, 2020.

[32] Angela Jinsook Oh, Tiffany Chen, Mohammad Ali Shariati, Naz Jehangir, Thomas N Hwang, and Yaping Joyce Liao, "A simple saccadic reading test to assess ocular motor function in cerebellar ataxia," *Plos one*, vol. 13, no. 11, pp. e0203924, 2018.

[33] JA Nij Bijvank, LJ Van Rijn, LJ Balk, HS Tan, BMJ Uitdehaag, and A Petzold, "Diagnosing and quantifying a common deficit in multiple sclerosis: Internuclear ophthalmoplegia," *Neurology*, vol. 92, no. 20, pp. e2299–e2308, 2019.

[34] Jenny A Nij Bijvank, Axel Petzold, Danko Coric, H Stevie Tan, Bernard MJ Uitdehaag, Lisanne J Balk, and Laurentius J van Rijn, "Quantification of visual fixation in multiple sclerosis," *Investigative ophthalmology & visual science*, vol. 60, no. 5, pp. 1372–1383, 2019.

[35] JA Nij Bijvank, A Petzold, LJ Balk, HS Tan, BMJ Uitdehaag, M Theodorou, and LJ Van Rijn, "A standardized protocol for quantification of saccadic eye movements: Demons," *PloS one*, vol. 13, no. 7, pp. e0200695, 2018.

[36] Feng Lu, Yusuke Sugano, Takahiro Okabe, and Yoichi Sato, "Adaptive linear regression for appearance-based gaze estimation," *IEEE transactions on pattern analysis and machine intelligence*, vol. 36, no. 10, pp. 2033–2046, 2014.

[37] Weston Sewell and Oleg Komogortsev, "Real-time eye gaze tracking with an unmodified commodity webcam employing a neural network," in *CHI'10 Extended Abstracts on Human Factors in Computing Systems*, pp. 3739–3744. 2010.

[38] Xucong Zhang, Yusuke Sugano, Mario Fritz, and Andreas Bulling, "Appearance-based gaze estimation in the wild," in *Proceedings of the IEEE conference on computer vision and pattern recognition*, 2015, pp. 4511–4520.

[39] Qiong Huang, Ashok Veeraraghavan, and Ashutosh Sabharwal, "Tabletgaze: dataset and analysis for unconstrained appearance-based gaze estimation in mobile tablets," *Machine Vision and Applications*, vol. 28, no. 5-6, pp. 445–461, 2017.

[40] Seonwook Park, Adrian Spurr, and Otmar Hilliges, "Deep pictorial gaze estimation," in *Proceedings of the European Conference on Computer Vision (ECCV)*, 2018, pp. 721–738.

[41] Manir Ahmed and Rabul Hussain Laskar, "Evaluation of accurate iris center and eye corner localization method in a facial image for gaze estimation," *Multimedia Systems*, pp. 1–20, 2021.

[42] Anjith George and Aurobinda Routray, "Fast and accurate algorithm for eye localisation for gaze tracking in low-resolution images," *IET Computer Vision*, vol. 10, no. 7, pp. 660–669, 2016.

[43] Fabian Timm and Erhardt Barth, "Accurate eye centre localisation by means of gradients.," *Visapp*, vol. 11, pp. 125–130, 2011.

[44] Leo Pauly and Deepa Sankar, "A novel method for eye tracking and blink detection in video frames," in *2015 IEEE International Conference on Computer Graphics, Vision and Information Security (CGVIS)*. IEEE, 2015, pp. 252–257.

[45] Sophie De Brouwer, Demet Yuksel, Gunnar Blohm, Marcus Missal, and Philippe Lefèvre, "What triggers catch-up saccades during visual tracking?," *Journal of neurophysiology*, vol. 87, no. 3, pp. 1646–1650, 2002.

[46] Lee Friedman, John A Jesberger, and Herbert Y Meltzer, "A model of smooth pursuit performance illustrates the relationship between gain, catch-up saccade rate, and catch-up saccade amplitude in normal controls and patients with schizophrenia," *Biological psychiatry*, vol. 30, no. 6, pp. 537–556, 1991.

[47] Nicolas Burra and Dirk Kerzel, "Meeting another's gaze shortens subjective time by capturing attention," *Cognition*, vol. 212, pp. 104734, 2021.

[48] Roy S Hessels, Chantal Kemner, Carlijn van den Boomen, and Ignace TC Hooge, "The area-of-interest problem in eyetracking research: A noise-robust solution for face and sparse stimuli," *Behavior research methods*, vol. 48, no. 4, pp. 1694–1712, 2016.

[49] Antonia Vehlen, Ines Spenthof, Daniel Tönsing, Markus Heinrichs, and Gregor Domes, "Evaluation of an eye tracking setup for studying visual attention in face-to-face conversations," *Scientific reports*, vol. 11, no. 1, pp. 1–16, 2021.

[50] "Depth camera d435," *https://www.intelrealsense.com/depth-camera-d435/*, Jan 2021.

[51] A Serra and RJ Leigh, "Diagnostic value of nystagmus: spontaneous and induced ocular oscillations," *Journal of Neurology, Neurosurgery & Psychiatry*, vol. 73, no. 6, pp. 615–618, 2002.

[52] Davis E. King, "Dlib-ml: A machine learning toolkit," *Journal of Machine Learning Research*, vol. 10, pp. 1755–1758, 2009.

[53] Diederik P Kingma and Jimmy Ba, "Adam: A method for stochastic optimization," *arXiv preprint arXiv:1412.6980*, 2014.

[54] Seonwook Park, Xucong Zhang, Andreas Bulling, and Otmar Hilliges, "Learning to find eye region landmarks for remote gaze estimation in unconstrained settings," in *Proceedings of the 2018 ACM Symposium on Eye Tracking Research & Applications*, 2018, pp. 1–10.

[55] Yihua Cheng, Feng Lu, and Xucong Zhang, "Appearance-based gaze estimation via evaluation-guided asymmetric regression," in *Proceedings of the European Conference on Computer Vision (ECCV)*, 2018, pp. 100–115.

[56] Michael F Land, "Eye movements of vertebrates and their relation to eye form and function," *Journal of Comparative Physiology A*, vol. 201, no. 2, pp. 195–214, 2015.

[57] Muhammad Qasim Khan and Sukhan Lee, "Gaze and eye tracking: Techniques and applications in adas," *Sensors*, vol. 19, no. 24, pp. 5540, 2019.

[58] Anuradha Kar and Peter Corcoran, "A review and analysis of eye-gaze estimation systems, algorithms and performance evaluation methods in consumer platforms," *IEEE Access*, vol. 5, pp. 16495–16519, 2017.

[59] Asim H Dar, Adina S Wagner, and Michael Hanke, "Remodnav: robust eye-movement classification for dynamic stimulation," *Behavior research methods*, vol. 53, no. 1, pp. 399–414, 2021.

[60] I Tobii Technology, "Timing guide for tobii eye trackers and eye tracking software," *White Paper.*, 2010.

[61] John H Pula and Carlen A Yuen, "Eyes and stroke: the visual aspects of cerebrovascular disease," *Stroke and vascular neurology*, vol. 2, no. 4, pp. 210–220, 2017.